

Application of Smart Temperature Information Material for The Evaluation of Heat Storage Capacity and Insulation Capacity of Exterior Walls

Chih-Yuan Chang, Jin-Chiuan Chang, San-Shan Hung, and Cheng-Jui Hsu

Abstract—The heat storage capacity of concrete in building shells is a major reason for excessively large electricity consumption induced by indoor air conditioning. In this research, the previously developed Smart Temperature Information Material (STIM) is embedded in two groups of exterior wall specimens (the control group contains reinforced concrete exterior walls and the experimental group consists of tiled exterior walls). Long term temperature measurements within the concrete are taken by the embedded STIM. Temperature differences between the control group and the experimental group in walls facing the four cardinal directions (east, west, south, and north) are evaluated. This study aims to provide a basic reference for the design of exterior walls and the selection of heat insulation materials.

Keywords—building envelope, sensor, energy, thermal insulation, reinforced concrete

I. INTRODUCTION

ACCORDING to The Institute of Energy Economics, Japan – IEEJ (2006), commercial and residential buildings account for about one third of global energy consumption [1]. In Taiwan, the combined electricity consumption of residential and commercial buildings amounts to 30% of the total electricity usage in building structures, which is the largest non-industrial source of consumption. A major portion of this usage comes from air conditioning required to lower the indoor temperature. Heat produced by domestic electrical appliances and residents themselves, direct solar radiation through windows, and heat conduction through walls, roofs, and glass are the main heat sources in a building. Since Taiwan is located on the border of tropical and subtropical climate zones, daily solar radiation is especially strong during the summer months. Therefore, undesired thermal energy storage is a major issue. The duration of heat storage in reinforced concrete (RC) buildings exceeds the normal length of the day (sunrise to sunset), and there is not enough time for the absorbed thermal energy to dissipate during the night. Consequently, mechanical airconditioning systems use a substantial amount of energy to maintain a comfortable indoor environment, and the associated cost is high [2]. Xiande Lin (2007) believes that energy saving strategies for buildings are more important than those for other disciplines and have a more profound influence due to the longer service life of buildings compared to other industrial products [3].

According to a calculation of air conditioning cooling load, heat from solar radiation that enters buildings through exterior walls and windows accounts for more than 30% of the total cooling load of the building [4]. Vijaykumar KCK et al. (2007) state that appropriate selection of exterior heat insulation materials is essential in reducing building air conditioning load [5]. The heat insulating and storage capacity of building exteriors depend on various characteristics of the material (heat conductivity, specific heat capacity, and density) as well as the climate [6]. In Taiwan, 77.6% of new buildings are constructed using reinforced concrete [7]. The exterior shells of these RC structures absorb much heat during the day as a result of the large heat storage capacity of concrete. Instead of cooling the internal environment and improving comfort through air conditioning during the operation stage (after the completion of the building), it is better to introduce exterior insulation into the building shells and assess its performance in the planning and design stage. Selection of the optimum insulation material so that heat from solar radiation is prevented from entering the building via the exterior shell has become an important research topic.

There are a number of investigations that use energy simulation software or calculate the material heat transfer coefficient U-values or heat resistance R-values to analyze building shell heat insulation capacity. The outcomes of these studies, which are based on indirect measurements, are very useful in the design stage of the building's life cycle. The present research utilizes STIM, which enables direct measurement, to achieve long term and continuous monitoring of thermal conditions within RC during the operation stage. It can provide an in-depth knowledge of the heat absorption and dissipation processes within concrete facing different directions. If analysis results from the direct measurements can be fed back to design architects, they can reduce the exterior wall thickness at appropriate places, and choose better exterior insulation material for walls with high heat absorption (e.g. those facing west or south).

This study uses Radio Frequency Integrated Circuit (RFIC) technology combined with temperature and humidity sensors. By designing a custom electronic circuit and package box, we have developed a smart temperature information material (STIM) which can be embedded into reinforced concrete, and is only 50mm×48mm×50mm in size. STIM is a new measurement technology that features direct measurement, wireless transmission, and real-time continuous monitoring [8]. A sealed but unpackaged STIM transmitter is shown in Fig.1. The user interface was designed in the Building Physiology Information System (BPIS) developed using the Borland C++

Assoc. Prof. Dr. Chih-Yuan Chang is with Feng Chia University, Taiwan
e-mail:rchang@fcu.edu.tw

Builder program. The BPIS contains database setup and user interface design. In addition to real-time monitoring of RC structures, it also records long term temperature measurements at all sensing points. BPIS can provide on-site building managers with real-time data at multiple points, abnormality alerts, and historical data [9]. In order to better understand the insulation capacity of various roof insulation materials, we insert STIM transmitters into five concrete specimens (50cm×50cm×15cm) representing designed roof insulation and conduct long term temperature monitoring [10]. The STIM and BPIS systems facilitate the evaluation of heat capacity of different insulation materials and their efficiencies in energy savings. This information provides architects and building managers with references for heat insulation material selection as well as for energy savings analyses of air conditioning systems. In low rise buildings, the majority of heat from solar radiation is transferred into the building through the roof. By comparison, in high rise buildings, the exposed exterior wall area far exceeds the roof area. This study is therefore extended to exterior walls as well. We hope to assess heat insulation efficiency by conducting long-term monitoring of the impact of sunlight on exterior walls facing different directions (east, west, south, and north). This research will provide a reference for material selection at the design or renovation stage as well as for the evaluation of the energy efficiency of building shells.



Fig. 1 A sealed but unpackaged STIM transmitter

II. APPLICATION OF RFIC WITH TEMPERATURE SENSORS FOR CONCRETE TEMPERATURE SENSING

Radio frequency (RF) technology has been experiencing rapid development in recent years. RFIC is the result of minimizing the size and power consumption of the electronic circuits used in RF technology. It differs from Radio Frequency Identification (RFID) for identity recognition in the field of intelligent buildings and construction management. RFIC's functions of sensing and monitoring relevant physical and chemical properties can be further enhanced by integration with specifically designed software, resulting in more flexibility in measurement and management. The application of RFIC technology can be extended to a large number of areas, e.g. monitoring of aircraft wing motion [11], temperature monitoring during the transport of captured fish and shellfish to the processing factory [12], use with various sensors to produce multi-agent design methods and system evaluation [13], and monitoring of real-time respiratory signals [14].

While it is not difficult to use RFIC technology in atmospheric temperature and humidity measurement, embedding it into reinforced concrete to take measurements proves difficult, and the combined application of RFIC and sensors is rarely researched. A few approaches involving direct measurement are adopted by some researchers including the following: the use of K or T type thermocouples to measure the surface temperature or the temperature of a central point inside the concrete specimen; the use of thermo-resistance or infrared thermal imaging technology to measure the temperature variation of building shells; mathematical derivation of the thermal transfer rate U-value, thermal resistance R-value, or temperature gradient to estimate the temperature inside the concrete panel; and the use of numerical modeling to evaluate the thermal properties of building shells and modification of the design accordingly [15]-[18]. Using the methods listed above, one can evaluate the heat penetration capacity of building exterior walls, measure temperature at a single point, or measure temperature variation at the surface. There is, however, an issue with the validity of this calculated or measured data, in that they do not account for dynamic variation, nor are they long term measurements. Moreover, reinforced concrete panels cannot be treated as homogeneously layered material (e.g. exterior insulating layer, paint layer, concrete layer, layer of reinforcing bars, fillings, etc.). Direct and continuous measurements, if they can be obtained, will offer a more reliable and valuable reference.

III. EXPERIMENTAL SETUP

The present research compares the heat insulation capacities of materials commonly used as building exterior walls in Taiwan, in hopes of providing useful references for future energy saving designs or for material selection in renovation of older building exteriors. Specimens of size 50cm×50cm×15cm are used to represent the exterior concrete panels. To prevent the ambient thermal environment from interfering with internal temperatures measured by STIM, the four sides and the bottom inside of the experiment box were covered with 1.5cm thick white polystyrene foam boards. The STIM is positioned in the center of the specimen, as shown in Fig.2. For specimens to receive the same amount of sunlight, and also to minimize human and environmental influences, the experiment must be conducted in a vast open space. The chosen site (refer to Fig.3) is located on the rooftop of Civil/Hydraulic Engineering Building at the Feng Chia University in Taichung City, Taiwan (latitude and longitude 120.646889E / 24.180974 N).

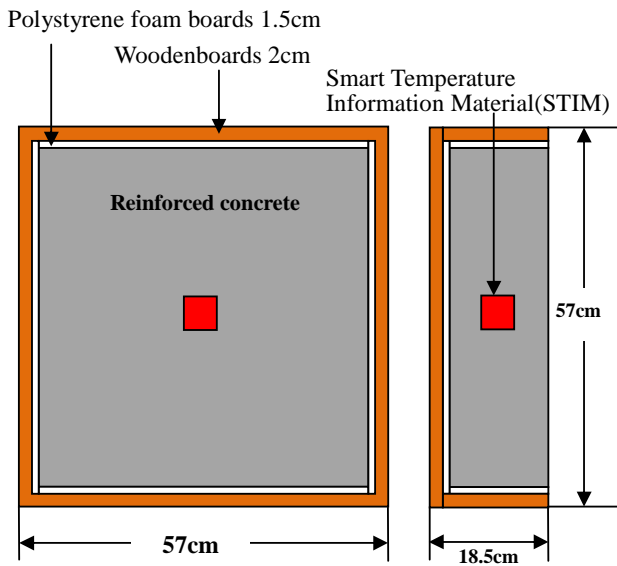


Fig. 2 STIM embedded in the concrete specimen



Fig. 3 Experiment site

To compare the thermal insulation capacity of different materials, two groups of reinforced concrete panel models, representing exterior walls, were prepared. The control group has no insulation material while the experimental group is covered with a type of ceramic tile which is commonly used in Taiwan as insulation material for exterior wall panels. Fig. 4 and 5 show models for the control group and the experimental group, respectively. Both models comprise four wall panels facing different directions so that temperature differences associated with different orientations can be investigated. Tiles in the experimental group are of the size 22.5cm x 6cm x 0.7cm each, as shown in Fig. 6. By continuously measuring temperature changes in the specimens of both groups and comparing differences between the two groups, we evaluate the heat insulation capacity of tiled exterior walls. The effect of building shell cooling through the use of the insulation material on air conditioning electricity consumption is analyzed.



Fig. 4 Control group consisting of reinforced concrete exterior walls



Fig. 5 Experimental group consisting of tiled exterior walls



Fig. 6 Exterior wall tiles used in the experimental group

IV. EVALUATION OF HEAT STORAGE CAPACITY OF EXTERIOR WALLS AND THE HEAT CAPACITY OF INSULATION MATERIAL

A. Effect of Sunlight and Orientation on The Heat Storage of Concrete Walls

The phenomenon of sunlight directly entering building blocks and falling on the surface of building exterior structures or indoors is called architectural daylighting. The sun rises in the morning from the east and sets in the west, so the solar angle on buildings is constantly changing throughout the day. Therefore, the heat absorption of exterior walls on the four sides of the building is different. In this experiment, we embed STIM transmitters (developed within our research group) into RC exterior wall panel specimens. For specimens in the

experimental group (insulation of tiles is not considered here), dynamic variation in the internal temperature of walls with different orientations is measured. The STIM measurement is configured to be taken every five minutes. The four exterior walls of the specimen are positioned to face the east, south, west, and north.

The embedded STIM unit continuously carries out internal temperature measurements over a long duration, and results are recorded in the BPIS database. Data taken in the period of 2011/09/23~2011/09/29 is used for discussion in this section. At that time, the season in Taiwan is early autumn.

The time when maximum temperature is observed in the panel differs with orientation. In general, atmospheric temperature reaches a daily maximum at around noon. The west wall of the specimen is not at its maximum internal temperature until 5 hours later, at 5pm in the afternoon. The hysteresis effect observed for time of maximum temperature in the four walls is shown in Fig. 7. Due to differing amounts of sunlight, the east wall reaches a maximum at the earliest time, followed by the south, north, and then west wall.

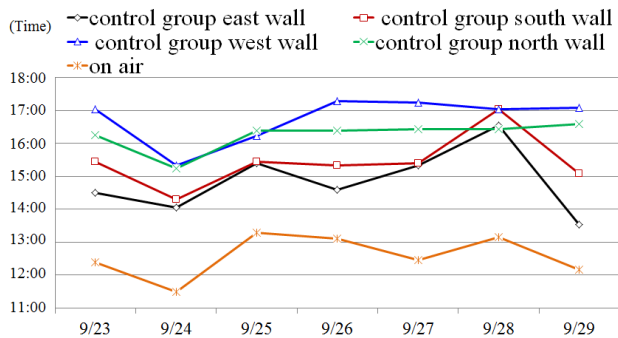


Fig. 7 The time of daily temperature peak in the four walls of the specimen in the experimental group

In the week shown in Figure 7, according to data from the Taiwan central weather bureau's monitoring station in Taichung, it was sunny on all days except for 2011/09/28 (rain) and 2011/09/24 (clouds).

The record shows that the maximum temperature inside the concrete usually lasts for 0.5~2 hours, unlike in the atmosphere where temperature dips immediately after the maximum is reached. For example, on 2011/09/23, the east wall reached a maximum temperature of 34.6° the earliest, at 14:49~15:55 according to STIM measurements; the south wall was next to reach its maximum of 38.9° at 15:24~16:24; the north wall reached a maximum of 32°, around 16:25~17:25; and the west wall recorded a maximum of 40.4° at 16:59~17:24.

When the west wall reached its maximum in the afternoon, the difference with atmospheric temperature at the same time was 12.3° (refer to Table I), which is remarkable. The 12.3° difference between the west wall of the specimen and the atmosphere explains why west facing houses in a building are not preferred by the general public. In the afternoon and evening, concrete exterior walls facing the west are still at a high temperature and continue to dissipate heat into the rooms. In some cases, air conditioning is necessary even in the evenings to lower the room temperature. This is a serious

challenge to energy savings and reduction of carbon emissions.

TABLE I
TIME OF TEMPERATURE RISE AT DIFFERENT ORIENTATIONS (DATE:
2011/09/23)

	East wall	South wall	West wall	North wall
Period of temperature rise in the concrete	am6:49~pm14:49	am7:19~pm15:24	am8:14~pm16:59	am7:34~pm16:25
Duration	8hrs	8.1hrs	8.75hrs	8.85 hrs
Start temperature	23.6°C	24.7°C	24.5°C	23.4°C
Maximum temperature (A)	34.6°C	38.9°C	40.4°C	32°C
Duration of the maximum temperature	1hrs	1hrs	0.5hrs	1hrs
Atmospheric temperature when (A) is reached, (B)	32.6°C	31.8°C	28.1°C	28.8°C
Difference between A-B	2°C	7.1°C	12.3°C	3.2°C

Buildings of different purposes have their own service times and frequencies of use. Buildings that are used often during the day include office buildings, schools, and factories, while residential buildings and department stores are used more frequently at night.

If the dynamic temperature variation within the concrete can be continuously monitored for more than a year, the results can provide valuable references for building designers or managers in the areas of space planning, energy savings and carbon reduction policies, exterior insulation design, and renovation planning. They can also assist with the design of Smart Skin used in intelligent buildings, in aspects such as dynamic heat insulation, increased shades or insulation at the west face, and automatic temperature adjustment function for exterior walls.

B. Effect of Weather and Climate on The Heat Storage of Concrete Walls

The relative motion of the sun and the earth is the reason for the distinction between day and night, and the division of the four seasons. In the northern hemisphere, days are longer than nights in summer and shorter in winter. In the spring and autumn, days and nights are similar in length.

In winter, the south receives the longest duration of sunlight, followed by the east and west, while the north receives almost no sunlight. In summer, due to the larger solar angle range, all orientations are exposed to sunlight. The east and west sides have more sunlight, followed by the south and the north. It can therefore be predicted that if the monitoring can continue for over a year, results in different seasons will vary.

Even in the same season, due to the distinct division of the four seasons in Taiwan, monthly data is expected to fluctuate. The autumn starts in September and ends in November, and the monitoring in this study begins in early autumn. Fig. 8 presents continuous measurements between 2011/09/23 and 2011/09/29. During this week, there were sunny days, cloudy days, and rainy days. One sample from each weather condition is taken. For example, one sample is taken on a sunny day (2011/09/26), one on a cloudy day (2011/09/24), and one on a

rainy day (2011/09/28). In the following discussion, we aim to examine the maximum temperature differences inside the concrete walls of specimen in the control group under three weather conditions in early autumn (September).

The four walls face the east, west, south, and north.

- 1) Sunny day sample: The maximum temperature of the day occurs at 17:29. The west wall of the specimen shows a recorded maximum internal temperature of 44.3°C, followed by the south wall which has a maximum of 42.6°C. The maximum temperature in the east wall is 38.7°C, and that in the north wall is 35.8°C. The temperature difference between the west and north walls is 8.5°C.
- 2) Cloudy day sample: The maximum temperature of the day occurs at 14:29. The south wall of the specimen shows a recorded maximum internal temperature of 36.3°C, followed by the west wall which has a maximum of 34.5°C. The maximum temperature in the east wall is 32.7°C, and that in the north wall is 31.8°C. The temperature difference between the south and north walls is 4.5°C.
- 3) Rainy day sample: The maximum temperature of the day occurs at 17:04. The west wall of the specimen shows a recorded maximum internal temperature of 32.2°C, followed by the south wall which has a maximum of 31.9°C. The maximum temperature in the east wall is 31.6°C, and that in the north wall is 31.5°C. The temperature difference between the west and north walls is 0.7°C.

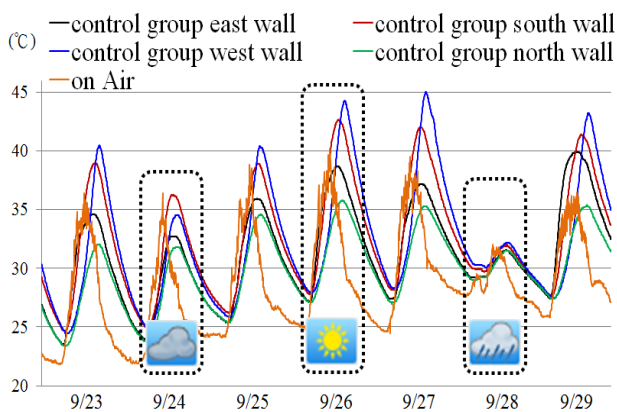


Fig. 8 Measurements under different weather conditions in September (control group)

Fig. 9 contains data from continuous monitoring between 2011/11/13 and 2011/11/19 (late autumn in Taiwan), during which there are sunny days, cloudy days, and rainy days. One sample from each weather condition is taken.

For example, one sample is taken on a sunny day (2011/11/14), one from a cloudy day (2011/11/13), and one from a rainy day (2011/11/17). We first discuss the maximum temperature differences within the concrete walls of the

specimen in the control group under three weather conditions in late autumn (November).

The four walls of the specimen face the east, west, south, and north.

- 1) Sunny day sample: The maximum temperature of the day occurs at 14:59. The south wall of the specimen shows a recorded maximum internal temperature of 39.7°C, followed by the west wall which has a maximum of 36.5°C. The maximum temperature in the east wall is 29.7°C, and that in the north wall is 26.9°C. The temperature difference between the south and north walls is 12.8°C.
- 2) Cloudy day sample: The maximum temperature of the day occurs at 15:34. The south wall of the specimen shows a recorded maximum internal temperature of 32.8°C, followed by the west wall which has a maximum of 32.1°C. The maximum temperature in the east wall is 27.3°C, and that in the north wall is 26.7°C. The temperature difference between the south and north walls is 6.1°C.
- 3) Rainy day sample: The maximum temperature of the day occurs at 15:04. The south wall of the specimen has a recorded maximum internal temperature of 28.5°C, followed by the west wall which has a maximum of 28.3°C. The maximum temperature in the east wall is 28.0°C, and that in the north wall is 27.3°C. The temperature difference between the south and north walls is 1.2°C.

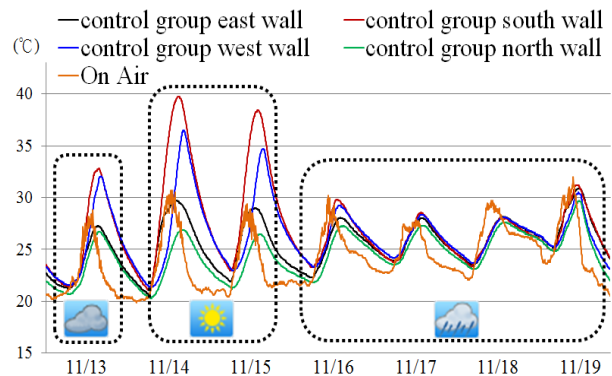


Fig. 9 Measurements under different weather conditions in November (control group)

The results show that due to the influence of sunlight on the internal temperature of concrete walls with different orientations under sunny weather in September, the temperature increase in the west face is higher than that in the south face. The east face has an even lower increase in temperature, and north face has the least increase. On sunny days in November, however, shorter days and longer nights result in less sunlight time for the west face. As a result, temperature rise in the south face is higher than that in the west. The east and north faces do not show significant seasonal differences in September and November (sample

from the sunny day). Regarding cloudy day samples, the ranking of maximum temperatures in the four faces stays the same as the November sunny day samples. There is no obvious temperature difference in different orientations under sunny and cloudy weather in November.

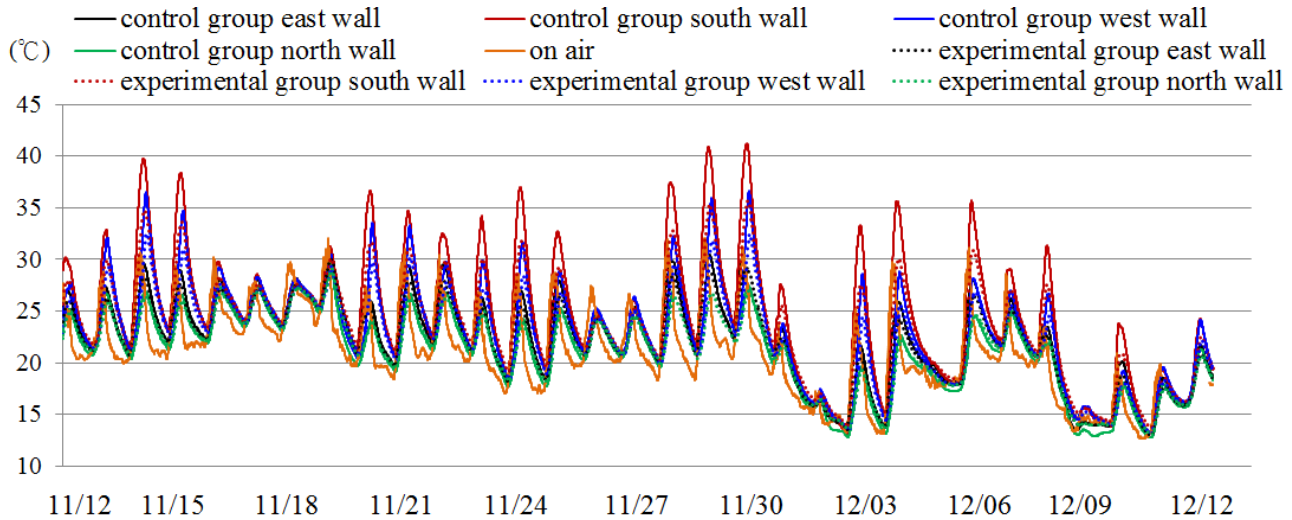


Fig. 10 Temperature change in the experimental group and the control group

Moreover, in both September and November, the difference in the maximum temperature for cloudy day samples is roughly half that for sunny day samples. On rainy days, there is very little temperature difference in both September and November because the concrete is not exposed to sunlight.

C. Effect of Heat Insulation Materials on The Heat Storage of Concrete Walls

To understand the thermal insulation capacity of the ceramic tiles commonly used on exterior walls in Taiwan, two groups of RC exterior wall specimens were prepared (refer to Fig. 4 and 5). The control group specimen shown in Figure 4 does not contain insulation material. The specimen of the experimental group in Figure 5 is covered with tiles. There are 8 wall panels in total for both specimens, each containing an embedded STIM transmitter for temperature monitoring (as shown in Fig. 2). These 8 STIM transmitters take simultaneous measurements of the dynamic temperature variation inside the specimens in both groups. Fig. 10 displays measured data for the month from 2011/11/12 to 2011/12/12. Samples include sunny, cloudy, and rainy weather during the month. The recorded results show that tiled specimens in the experimental group (dashed line) clearly have less variation in temperature compared to the control group (solid line). Measurements of a sample from a sunny day (2011/11/14) in the month are shown in Fig. 11.

We compare the difference associated with orientations in both the control and the experimental groups below:

- 1) South face of the specimen: The maximum temperature of 39.7°C occurs between 14:59 and 15:44 in the control group. The average atmospheric temperature during this time is 27.8°C, which gives an 11.9°C difference. The tiled specimen in the experimental group experiences its maximum temperature of 34.7°C between 15:51 and 16:26. The average atmospheric temperature during this period is 26.7°C, which gives a difference of 8°C. The maximum temperature in the experimental group occurs about one hour later than in the control group. The maximum difference between the two groups is 5°C (39.7°C - 34.7°C). In short, exterior insulation material (tiles) can at most resist heat equivalent to 5°C at the time of the experiment.
- 2) West face of the specimen: The maximum temperature of 36.5°C occurs between 16:44 and 17:04 in the control group. The average atmospheric temperature during this period is 25.0°C, which gives an 11.5°C difference. The tiled specimen in the experimental group experiences its maximum temperature of 32.5°C between 17:06 and 17:31. The average atmospheric temperature during this time is 24.1°C, which gives a difference of 8°C. The

maximum temperature in the experimental group occurs about one hour later than in the control group. The maximum difference between the two groups is 4°C. These results indicate that the influence of insulation material resembles that on the south face of the model.

- 3) East face of the specimen: The maximum temperature of 29.7°C occurs between 14:15 and 15:04 in the control group. The average atmospheric temperature during this period is 28.7°C, which gives a 1°C difference. The tiled specimen in the experimental group experiences its maximum temperature of 28.2°C between 14:42 and 16:37. The average atmospheric temperature during this time is 27.3°C, which gives a difference of 0.9°C. The maximum temperature in the experimental group occurs about half an hour later than in the control group. The maximum difference between the two groups is 1.2°C. It is clear that the insulation material does not make much of a difference on the east face.
- 4) North face of the specimen: The maximum temperature of 26.9°C occurs between 16:00 and 17:10 in the control group. The average atmospheric temperature during this period is 25.8°C, which gives a 1.1°C difference. The tiled specimen in the experimental group experiences its maximum temperature of 26.4°C between 16:42 and 17:17. The average atmospheric temperature during this time is 24.7°C, which gives them a difference of 1.7°C. The maximum temperature in the experimental group occurs about half an hour later than in the control group. The maximum difference between the two groups is 0.5°C. These results indicate that the effect of insulation material resembles that on the east face of the specimen.

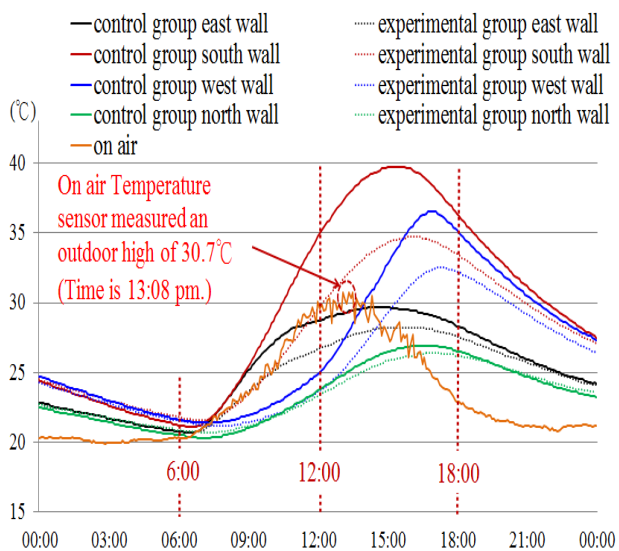


Fig. 11 Heat insulation capacity of the insulation material at different orientations

During the day, atmospheric temperature is often higher in the afternoon than it is in the morning. The same pattern exists inside the concrete exterior walls. In addition to the atmospheric temperature, thermal conditions inside the exterior concrete are also affected by the solar angle. Therefore, temperatures in concrete walls facing different directions begin to rise at different times. The average temperatures, which are equivalent to heat resisted by the insulation material, in the morning (6:00~11:59) and in the afternoon (12:00~17:59) for both the tiled experimental group and the control group are tabulated below:

TABLE II
EFFECT OF WEATHER AND ORIENTATION ON THE HEAT INSULATION CAPACITY OF THE INSULATION MATERIAL

Weather	Average ΔT	East face	South face	West face	North face
Sunny day sample (2011/11/14)	Morning	1.19°C	1.80°C	0.52°C	-0.13°C
	Afternoon	1.48°C	5.01°C	3.08°C	0.58°C
Cloudy day sample (2011/11/13)	Morning	0.36°C	0.21°C	0.57°C	-0.08°C
	Afternoon	0.95°C	2.82°C	2.50°C	0.82°C
Rainy day sample (2011/11/26)	Morning	0.25°C	0.03°C	0.49°C	-0.18°C
	Afternoon	0.74°C	0.54°C	1.01°C	0.43°C

The morning and afternoon average ΔT values in Table 2 are calculated as follows: taking the morning slot (6:00~11:59) as an example, measurements are taken every half hour. So there are 12 such data points in the morning, the average of which is denoted ΔT . This ΔT describes the average temperature, which is equivalent to the heat the thermal insulation material is capable of resisting within the time period (6 hours in the morning or in the afternoon).

- 1) Sunny day sample (2011/11/14): In the morning, the south face has the maximum heat resistance, followed by the east face. The temperature difference in the west face is below 1°C, and is negative for the north face. This means that despite the increased atmospheric temperature in the morning, tiles on the north face of the specimen play the

role of heat storage, not heat resistance. In the afternoon, the south face also resists the most heat. The temperature difference is more obvious in the west face than in the morning due to its exposure to direct sunlight. The temperature in the concrete at the east face starts to decrease in the afternoon. As a result, the temperature difference is similar to that in the morning. The temperature difference in the north face is larger than in the morning. However, the main heat source is the atmosphere, not solar radiation. Therefore, the difference is not apparent, all below 1°C.

- 2) Cloudy day sample (2011/11/13): In the morning, the west face has the maximum heat resistance, followed by the east and south faces. The temperature differences in all three faces are below 1°C, and it is negative in the north face. This means that tiles in the north face of the specimen keep the heat in the concrete at a lower ambient temperature. In the afternoon, the south face has the maximum heat resistance. The temperature difference is more obvious in the west face than in the morning due to its exposure to direct sunlight. The temperature differences in the east and north faces are larger than those in the morning. However, the heat mainly comes from the atmosphere rather than from solar radiation. Therefore, the difference is not obvious.
- 3) Rainy day sample (2011/11/26): The temperature differences in the afternoon are larger than those in the morning for all four faces. The main heat source is the atmosphere, not solar radiation. Therefore, the heat insulation effect of the insulation material is not prominent, and temperature differences are all below 1°C. A negative difference occurs in the north face in the morning. This indicates that tiles in the north face of the specimen preserve the heat in the concrete at lower ambient temperature.

V. CONCLUSIONS AND SUGGESTION

In the future, research groups can make more use of innovative sensing technology such as STIM to directly measure the dynamic temperature changes inside building exterior walls. When a sufficient amount of monitoring data is collected, statistical and comparison analyses can be performed on the temperatures in the database according to various criteria such as environment, location, exterior wall pattern, and orientation. It is believed that this can provide more accurate information regarding concrete heat storage capacity.

It will also enable building designers to comprehensively consider factors including the latitude and longitude of the building location, weather conditions, and the geographical environment in orientation design and space planning. There is a distinct division between seasons in Taiwan, and weather varies significantly. Therefore, it is possible to understand, in a short period of time, the influence of weather and seasonal variations on the temperature changes inside the concrete. If continuous monitoring of temperature variations within the

concrete can last over a year and the results are compared and evaluated across four seasons, it can provide more valuable references for architects in the selection of optimal orientation, selection of exterior thermal insulation material, and assessment of energy consumption in indoor air conditioning.

Due to the limitations of research funding and time, this research only investigated the application of STIM in the evaluation of the performance of thermal insulation materials. Further work can be carried out on the effect of orientation on the heat absorption and dissipation time, and associated differences in the temperature variation. Without compromising structural safety, exterior wall thickness can be adjusted (e.g. thick reducing from 15cm to 8cm) at the design stage, or thermal insulation capacity can be enhanced for insulation material on the west and south faces, where large heat absorption occurs.

Moreover, STIM can also be introduced into the building shell facade to develop Smart RC skin with an automatic temperature adjustment function. This can effectively prevent heat from being transferred into the indoor environment due to excessive heat accumulated in the exterior concrete walls, thus reducing unnecessary energy consumption in the building.

ACKNOWLEDGEMENTS

The research team acknowledges with gratitude the 2010 research grant issued by National Science Council (Project no: NSC 100-2221-E-035-092-)

REFERENCES

- [1] The Institute of Energy Economics, Japan, <http://eneken.ieej.or.jp/en/> (accessed on 9 October 2011).
- [2] J. L. Alvarado, W. Terrell, and M. D. Johnson, "Passive cooling systems for cement-based roofs," *Build. Environ.*, vol.44, no. 9, pp. 1869-1875, Sep. 2009.
- [3] H. T. Lin, Energy efficiency design of building envelopes and Strategies for reducing CO₂ emission, Architecture and Building Research Institute, Ministry of the Interior, 2007. pp. 15-34.
- [4] D. C. Chou and J. J. Chiou, "A Study on the Insulation Performance of a Double Skin Roof Induced by Natural Ventilation," *Journal of Architecture*, no.59, pp.79-92, 2007.
- [5] K. C. K. Vijaykumar, P.S.S. Srinivasan, and S. Dhandapani, "A performance of hollow clay tile (HCT) laid reinforced cement concrete (RCC) roof for tropical summer climates," *Energy Build.*, vol. 39, no. 8, pp. 886-892, Aug. 2007.
- [6] A. Praditsmanont, and S. Chungpaibulpatana, "Performance analysis of the building envelope: A case study of the Main Hall, Shinawatra University," *Energy Build.*, vol.40, no. 9, pp.1737-1746, 2008.
- [7] C. Y. Chang, W. H. Hsiao, S. M. Huang, and S. J. Guo, "Supply and Demand for Building Health Check," *Journal of Architecture*, no.59, pp.93-112, 2007.
- [8] C. Y. Chang, and S. S. Hung, "Implementing RFIC and sensor technology to measure temperature and humidity inside concrete structures," *Constr. Build. Mater.*, vol. 26, no. 1, pp. 628-637, Jan. 2012.
- [9] C. Y. Chang, S. S. Hung, Y. F. Peng, W. T. Chang, and H. Y. Feng, "Building Physiology Information System for Health Monitoring in Reinforced Concrete Structures", *Intelligent Buildings International*, DOI:10.1080/17508975.2011.642477
- [10] C. Y. Chang, S. S. Hung and Y. F. Peng, "An Evaluation of the Embedment of a Radio Frequency Integrated Circuit with a Temperature Detector in Building Envelopes for Energy Conservation," *Energy Build.*, vol. 43, no. 10, pp.2900-2907, Oct. 2011.
- [11] X. L. Zhao, T. Qian, G. Mei, C. Kwan, R. Zane, C. Walsh, T. Paing, and Z. Popovic, "Active health monitoring of an aircraft wing with an embedded piezoelectric sensor/actuator network: II Wireless approaches," *Smart Mater. Struct.*, vol.16, no. 4, pp. 1218-1225, Aug. 2007.
- [12] K. Crowley, J. Frisby, S. Murphy, M. Roantree, and D. Diamond, "Web-based real-time temperature monitoring of shellfish catches using a wireless sensor network," *Sens. Actuator A-Phys.*, vol. 122, no. 2, pp. 222-230, Aug. 2005.
- [13] J. Wu, S. F. Yuan, S. Ji, G.Y. Zhou, Y. Wang, and Z. L. Wang, "Multi-agent system design and evaluation for collaborative wireless sensor network in large structure health monitoring," *Expert Syst. Appl.*, vol. 37, no. 3, pp. 2028-2036, Mar. 2010.
- [14] N. Andre, S. Druart, P. Gerard, R. Pampin, L. Moreno-Hagelsieb, T. Kezai, L.A. Francis, D. Flandre, J.P. Raskin, "Miniaturized Wireless Sensing System for Real-Time Breath Activity Recording," *IEEE Sens. J.*, vol. 10, no. 1, pp. 178-184, Jan. 2010.
- [15] R. U. Halwatura, and M.T.R. Jayasinghe, "Thermal performance of insulated roof slabs in tropical climates," *Energy Build.*, vol. 40, no. 7, pp. 1153-1160, 2008.
- [16] F. Stazi, C. Di Perna, and P. Munafo, "Durability of 20-year-old external insulation and assessment of various types of retrofitting to meet new energy regulations," *Energy Build.*, vol. 41, no. 7, pp. 721-731, Jul. 2009.
- [17] S. A. Al-Ajlan, "Measurements of thermal properties of insulation materials by using transient plane source technique," *Appl. Therm. Eng.*, vol. 26, no. 17-18, pp. 2184-2191, Dec. 2006.
- [18] H. L. Zhang, W. M. Marci, and X. Z. Fu, "Modeling of the hydrothermal absorption and desorption for underground building envelopes," *Energy Build.*, vol. 42, no. 8, pp. 1215-1219, Aug. 2010.